Aneulysis - A System for Aneurysm Data Analysis

M. Meuschke[1,2], R. Wickenhöfer[3], B. Preim[1], K. Lawonn[2]

[1]Department of Simulation and Graphics, University of Magdeburg, Germany
[2]Institute of Computer Science, University of Jena, Germany
[3]Herz-Jesu Krankenhaus Dernbach, Germany

Abstract
We present ANEULYSIS, *a system to improve risk assessment and treatment planning of cerebral aneurysms. Aneurysm treatment must be carefully examined as there is a risk of fatal outcome during surgery. Aneurysm growth, rupture, and treatment success depend on the interplay of vascular morphology and hemodynamics. Blood flow simulations can obtain the patient-specific hemodynamics. However, analyzing the time-dependent, multi-attribute data is time-consuming and error-prone.* ANEULYSIS *supports the analysis and visual exploration of aneurysm data including morphological and hemodynamic attributes. Since this is an interdisciplinary process involving both physicians and fluid mechanics experts, we provide a redundancy-free management of aneurysm data sets according to a consistent structure. Major contributions are an improved analysis of morphological aspects, simultaneous evaluation of wall- and flow-related characteristics as well as multiple attributes on the vessel wall, the assessment of mechanical wall processes as well as an automatic classification of the internal flow behavior. It was designed and evaluated in collaboration with domain experts who confirmed its usefulness and clinical necessity.*

CCS Concepts
• *Computing methodologies* → *Collision detection;* • *Hardware* → *Sensors and actuators; PCB design and layout;*

1. Introduction

Cerebral aneurysms are pathological dilatations of intracranial arteries. Aneurysm rupture leads to internal bleeding causing high risk of mortality. Although most aneurysms will never rupture, the potential risk of bleeding makes their detection and risk-assessment a critical issue. The decision to treat a non-ruptured aneurysm involves a patient-specific risk analysis [CMWP11].

Aneurysm initiation, evolution, and rupture are caused by several factors, such as genetics, vessel morphology, inflammation, hemodynamics and epidemiological factors such as gender and age. In clinical routine, aneurysm risk assessment and treatment planning are based on medical guidelines that consider only morphological features such as aneurysm location, size, and shape [Ste11]. However, these attributes allow no reliable estimation of individual risk. Quantitative hemodynamic characteristics such as wall shear stress (WSS) or pressure as well as qualitative features, e.g., vortices seem to influence the aneurysm state including wall stability and thrombus formation [CMWP11]. Therefore, information on patient-specific hemodynamics is needed.

Computational fluid dynamics (CFD) simulations and fluid-structure interaction (FSI) can model the patient-specific wall mechanics and hemodynamics [JBB*13]. Both methods result in time-dependent flow data, comprising *scalar*, *vectorial* and *tensor-based* information, representing one cardiac cycle. In recent years, the investigation of hemodynamic information has become increasingly important due to improved image modalities and higher computer performance, which results in more accurate modeling of blood flow behavior. Based on these data, biomedical researchers compared ruptured and non-ruptured cases as well as different treatment options whether there are risky correlations between morphological and hemodynamic features. However, the visual exploration of the complex data is time-consuming and challenging. Gaining knowledge from simulated data requires customized analysis software that offers guided exploration through the different data types and is easy to use. Moreover, *standardized* data set evaluation is crucial to compare results from different research facilities.

Therefore, we present ANEULYSIS – an interactive management and visualization system to evaluate the rupture risk and treatment decisions of cerebral aneurysms. ANEULYSIS allows a consistent documentation and guided exploration of aneurysm data. Based on different modules, morphological and hemodynamic information comprising *scalar*, *vector*, and *tensor data* together with the internal blood flow can be analyzed simultaneously. We examine design decisions in the processing and evaluation pipeline, which were developed in close cooperation with neuroradiologists and CFD experts. Instead of introducing new attributes or assessment methods, we describe an *integrated system* for aneurysm management. We believe that an integrated system with powerful exploration and report functions is essential to reduce the gap between simulation and visual research, on the one hand, and clinical practice, on the other.

2. Related Work

The research of the rupture risk and treatment of cerebral aneurysms covers three main areas: the analysis of morphological aspects, the exploration of flow patterns, and the simultaneous investigation of morphological and hemodynamic aspects. While we focus on works dealing with the analysis of cerebral data, Oeltze et al. [OJMN*19] give an overview about the evaluation of medical flow data comprising cardiac, cerebral, and nasal data.

2.1. Analysis of Vascular Morphology

In clinical routine, aneurysms are classified using morphological aspects to assess the rupture risk and the associated need for treatment. Based on the ostium, the separating area between the healthy vessel part and the aneurysm, medical studies [DTM*08, LBM12] derived several morphological descriptors. Statistically significant differences between ruptured and non-ruptured aneurysms were detected. However, such descriptors allow no reliable risk estimation of asymptomatic aneurysms.

2.2. Analysis of Internal Blood Flow

Specific flow patterns, such as vortices, are considered as an indicator of pathologies [CMWP11] and are assumed to be related to treatment success [LAM*13]. To investigate their influence on pathological changes, medical studies are performed to determine in which vessel sections and phase of the cardiac cycle vortices occur. Such a classification is manually performed with common flow visualizations, which is a time-consuming and error-prone process. To support blood flow analysis, Lawonn et al. [LGP14b] presented a view-dependent approach that emphasizes automatically determined flow patterns. Besides partitioning techniques are used to decompose the flow into regions of common structure. Based on this, flow representatives can be computed and aggregated in a visual summary or a subsequent visualization can be restricted to specific regions, e.g., vortices. There are user-guided [GLvP*12] or automatic [OLK*14] approaches to perform the partitioning. Less frequently, local flow vectors [vPJtHRV12] or aneurysm wall properties [NLB*13] are employed.

Line predicates (LP) [SS06] are Boolean functions, employed in user-guided techniques, to partition integral curves into sets of similar behavior. Gasteiger et al. [GLvP*12] used LP to extract flow features in cerebral aneurysms. In contrast, automatic techniques utilize clustering methods to group integral curves based on a similarity measure. Oeltze et al. [OLK*14] compared multiple streamline clustering approaches for aneurysm flow and employed the best method to compare different stenting scenarios in which a metal implant is inserted into the parent artery to prevent blood from entering the aneurysm. Furthermore, Oeltze-Jafra et al. [OJCJP16] proposed a clustering-based visual analysis of vortical flow in cerebral aneurysms. They presented a pipeline for the automatic detection and visualization of *embedded vortices* forming around so-called *saddle-node bifurcations*. However, existing similarity measures are based on geometrical features between streamlines, where the temporal blood flow component is not directly considered. Two geometrically similar path lines occurring in non-overlapping time intervals would have a high similarity.

2.3. Analysis of Vessel Morphology and Hemodynamics

Gasteiger et al. [GNBP11] introduced the *FlowLens*, an interactive focus-and-context approach for the simultaneous exploration of anatomical and vectorial flow data. However, outside the lens area, the flow cannot be observed. To improve this, Lawonn et al. [LGP14a] employed a shading technique that visualizes morphological changes while simultaneously depicting blood flow. Neugebauer et al. [NLB*13] developed a qualitative exploration of near-wall hemodynamics, which is an important indicator for pathological vessel dilation. Lawonn et al. [LGV*15] presented a framework to analyze wall thickness with animated flow data using illustrative and cut-away techniques. Often, cerebral aneurysms are treated with a stent, where the neuroradiologists have to decide where the stent should be placed. Van Pelt et al. [vPGL*14] developed comparative visualization techniques revealing differences in the interplay of blood flow and wall mechanics based on possible stent configurations. For detailed overviews of illustrative and and cut-away techniques, we refer to [LP16, LVPI18, LSBP17].

Besides, several works generate more abstract representations of the 3D aneurysm surface to simplify data analysis. Neugebauer et al. [NGB*09] employed a multi-perspective 2D projection map for a combined exploration of the aneurysm morphology and hemodynamics. Goubergrits et al. [GSK*12] mapped the aneurysm to a uniform sphere to analyze statistical WSS distributions. Tao et al. [THQ*16] presented the *VesselMap*, a 2D mapping of an aneurysm and parent vasculature formulated as a graph layout optimization problem.

2.4. Software

Various free or commercial tools exist for the simulation and visual exploration of cerebral aneurysm data. ANKYRAS (commercial) by GALGOMEDICAL allows a patient-specific treatment planning based on different stent devices [NBR*18]. After the interactive implantation of a stent, the blood flow is simulated, where stent characteristics can be analyzed. *Syngo iFlow* (commercial) by Siemens Healthcare focused on the visual exploration of DSA data in a color-coded single image, where flow curves can be computed for interesting regions [CDJ*17]. It also allows a comparison of blood flow information in selected regions pre- and post-intervention [SLG15, ZMSL13]. *EnSight* (commercial) by Ansys is a software tool for post-processing and visualizing simulation data using standard techniques, such as color-coding forces on the vessel wall and particle animations to represent the inner blood flow. Different data sets can be compared using multiple views. *VMTKLab* by Orobix (commercial) allows an image-based generation of vascular models and simulation of the internal blood flow, which is visualized by particle animations [GRC*18]. *ParaView* (open source) is an application to visually analyze scientific data using qualitative and quantitative techniques [AGL05]. Similar to *EnSight* standard visualization methods are provided to explore simulation results.

Unfortunately, there are no systems that focus on the simultaneous analysis of wall and flow features including *scalar*, *vectorial*, and *tensor* data. Moreover, an objective analysis of blood flow patterns is missing. In addition, the storage of findings and automatic report generation have hardly been considered, which hampers the collaborative analysis and documentation.

3. Requirement Analysis

We closely cooperated with two neuroradiologists (16 and 25 years of work experience), who regularly treat cerebral aneurysms, and two engineers working on CFD simulations for cerebral aneurysms (five and eight years of work experience). The goal of the neuroradiologists is to assess the rupture risk, which requires a better understanding of risk factors. This also includes a comparison of ruptured and non-ruptured cases. In contrast, for the CFD engineers, it is important to validate the physical plausibility of the simulation results. For this purpose, they analyze fluid-wall interactions by exploring scalar quantities on the vessel wall and try to find spots of interesting combinations. This verification process also includes a determination of the most dominant flow patterns based on different boundary conditions for simulation.

Both types of experts use similar concepts and techniques to manage and analyze aneurysm data. For each data set, different kind of information for different points in time, i.e., pre- and post-operative data, are available. The data is stored on a server, where quantitative information such as morphological descriptors are stored in Microsoft Excel tables. Morphological descriptors are determined manually from 2D image slices using clinical software, or from 3D surfaces using *ParaView*. Both procedures are described as time-consuming by the experts. Scalar quantities, e.g., WSS or pressure, are color-coded on the 3D vessel surface to examine the aneurysm state. However, the experts consider the sole presentation of a 3D model as not sufficient since important information can be occluded. The blood flow is depicted either by streamlines or by path lines as an animation over the cardiac cycle. Based on such standard flow visualizations, the experts manually classify flow patterns according to pre-defined types such as in the study by Cebral et al. [CMWP11]. However, this is a time-consuming process with high inter-observer variability. Since the surface morphology and flow behavior influence each other, an integrated view of both characteristics is needed. At the moment, the aneurysm surface is depicted semi-transparently and animated path lines represent the blood flow. However, this makes it challenging to identify relationships between wall and flow characteristics.

Besides the individual exploration of aneurysm data by one expert, a collaborative analysis would be essential to improve the exchange of information. This would require a consistent storage structure of the data. Moreover, searching for specific cohorts is cumbersome, e.g., female patients with a ruptured aneurysm larger than 7 mm. However, this is relevant for medical studies to investigate risk factors. Based on a literature review and the discussions with our domain experts, we summarize significant requirements as follows:

Req. 1. A consistent and efficient data management. A consistent structure for data management is needed that allows fast integration of new data sets, including different meta information and data files. Moreover, information about existing data sets should be easily editable, and filter techniques are needed to select cohorts according to specific criteria.

Req. 2. Automatic feature extraction. Feature filtering should be supported by automatic methods to compute morphological descriptors as well as to extract and classify qualitative flow features, which ensures comparability and reproducibility of the results.

Req. 3. A comparison of data sets. Some particularly frequent comparisons should be directly supported, e.g., the comparison of ruptured and non-ruptured data sets as well as pre- and post-treated data including different stent scenarios.

Req. 4. Simplified visualizations. To reduce the complexity of 3D time-dependent aneurysm data, simplified depictions of the aneurysm morphology and internal flow are needed.

Req. 5. Integrated flow visualizations. Aneurysm flow data comprise *scalar*, *vectorial*, and *tensor* information. This information should be visualized in an integrated manner to allow a detailed analysis of possible rupture-prone configurations.

Req. 6. Overview of suspicious wall regions. The user should get an overview of suspicious wall regions over the cardiac cycle that require closer examination to reduce the manual exploration effort and to reduce the risk of overlooking something important. For this purpose, an automatic camera movement passing interesting vessel regions should be provided.

Req. 7. Collaboration tools. For collaboration purposes, it should be possible to set landmarks in different time steps. An external researcher should be able to analyze the regions around the landmarks and discuss them with other colleagues.

4. Data Acquisition and Pre-Processing

This section describes the data acquisition and pre-processing steps to simulate the flow within cerebral aneurysms. Major steps are the image acquisition, surface reconstruction, calculation of flow data and virtual stenting.

Image acquisition. First, clinical image data comprising CTA, MRA, and DSA of the aneurysm morphology are acquired.

Surface reconstruction. Based on the image data, the vessel surface is reconstructed using the pipeline by Mönch et al. [MNP11]. The aneurysm and its parent vessel are separated from the surrounding tissue using a threshold-based segmentation. The 3D vessel surface is extracted via *Marching Cubes*, applied to the segmented image data. To prepare a geometric model as input for the flow simulation, it is necessary to manually correct artifacts (see Mönch [MNP11]). Moreover, the mesh quality was optimized by a combination of metric and topological changes [Sch97].

Virtual stenting. To simulate different treatment scenarios, a fast virtual stent deployment was chosen [BDJ17]. This explicit methodology allows for the consideration of each stent strut and is superior compared to other approaches, e.g., based on a porous medium that represents the stent. Due to the usage of geometric deformation, this method can be applied within seconds without being computationally expensive.

CFD simulation. The pre- and post-treated meshes were spatially discretized using a combination of tetrahedral and prismatic cells. An appropriate grid size was chosen to obtain simulation results that would not be significantly changed by an improved resolution [JBB*13]. The conservation of mass and momentum is solved locally within each time step, where blood is assumed as an incompressible Newtonian fluid with a density of 1055 kg/m^3 and a dynamic viscosity of 0.004 $Pa\dot{s}$ [SAC*13]. Flow measurements of

a healthy volunteer are used as inlet boundary conditions due to the absence of patient-specific data. Zero pressure boundary conditions were applied at each outlet cross-section. In every case, three cardiac cycles with a time step size of $\delta t = 0.001s$ are simulated. To avoid inaccuracies from initialization, only the last cycle was used for analysis. Hemodynamic simulations were carried out using the solver *STAR-CCM+ 11*.

FSI simulation. Addressing the FSI simulation, every aneurysm is divided into two subdomains: the fluid and solid domain. Hemodynamic aspects inside the fluid domain are numerically solved using CFD. Furthermore, structural simulations are performed to include the vessel wall behavior. For this purpose, the deformable wall is considered as homogeneous, isotropic and linear elastic. The Young's modulus (1mPa) and Poisson's ratio (0.45) are taken from [VLR*08]. Wall thickness is set in the range of 0.2 to 0.6mm obtained by normal extrusion of the wall [VLR*08], because such data cannot be extracted yet from radiologic image data. To prevent rigid body motion, the vessel in- and outlet cross-sectional planes are fixed. The relation of deformation, mechanical strain, and mechanical stress is solved locally for each finite element, based on the conservation of momentum. The deformation of the solid domain reacts on the fluid domain and therefore on the flow characteristics, inducing a complex coupling of both domains. This coupling is located at the intersecting surface of fluid and solid. Thus, FSI is implemented as data transfer at the interface, exchanging fluid pressure as well as WSS and wall displacement, respectively as updated boundary conditions at defined time steps.

Post-processing. This includes the mapping of cell-based variables to the vertices of the surface mesh. Moreover, path lines are emitted at the cross-sectional area where the fluid enters the solid domain with an adaptive fifth order Runge-Kutta method. The integration is performed every 0.01s.

5. ANEULYSIS - Aneurysm Analysis System

This section describes the main components of ANEULYSIS as well as the guided management and visual analysis of aneurysm data.

Basically, the system consists of three components: a database, an FTP-server and a visualization component. To meet Req. 1, the acquired raw data and representations derived from it are stored on the FTP-server using a consistent structure that avoids redundancy. For each patient, a new case is created on the server, with pre- and post-treated data that is organized in studies. Each study comprises four information elements. *Scanner data* includes different image modalities such as CTA and MRA data. *Geometric information* is stored in reconstruction data, e.g., the ostium and centerline. Moreover, *flow simulations* are stored, for either single (steady) or multiple (unsteady) time steps. Here, also integration results in the form of stream or path lines are stored. *Media data* contains characteristic images or videos, e.g., showing wall regions with higher risk.

Furthermore, *metadata* is stored for the cases, studies and corresponding data items in the database. This includes, e.g., the study type (patient or proband), gender and age. Besides, more detailed information about the pathology, e.g., the location of an aneurysm, the number of existing aneurysms or information about rupture and treatment are collected in the database.
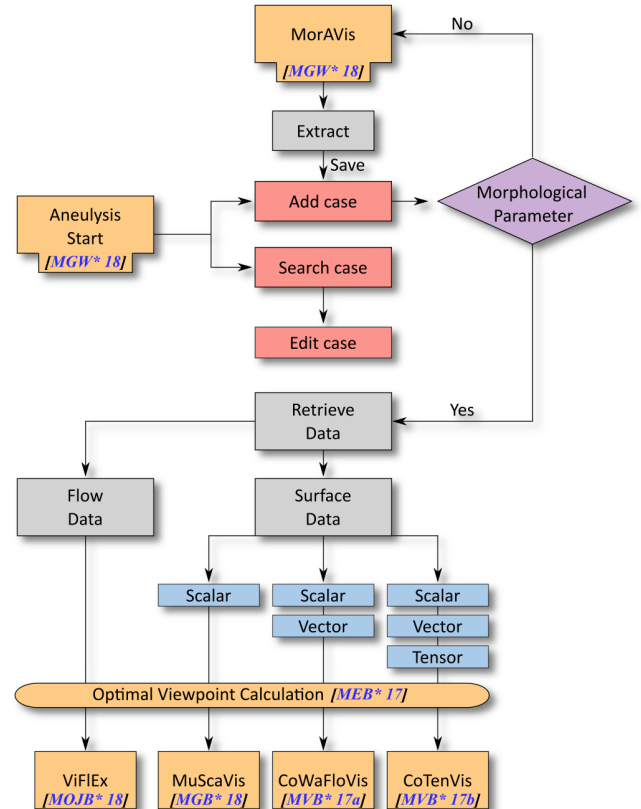

Figure 1: *Overview of the workflow with* ANEULYSIS.

There are three types of data for a selected data set: a surface representation showing the vessel morphology, wall-related information comprising scalar, vectorial, and tensor data defined on the vessel surface and flow-related information specified within the vessel lumen describing the internal blood flow. These three types of data are used as input for the visualization component. The visualization component consists of five modules, where each communicates with the database and the server to store results such as screenshots from the visual analysis.

5.1. General Workflow of Aneulysis

We provide a *guided workflow*, where domain experts can analyze data sets collaboratively. The guidance was realized on the main screen, where several processing screens are enabled depending on the previous user action. The collaboration was realized by the redundancy-free data management. Moreover, the user can place landmarks within the individual views, e.g., on the 3D vessel surface (Req. 7). Each landmark gets an individual color, and an individual label can be set. Thus, a textual description of each landmark is available, e.g., for documentation. After the placement, a screenshot is taken, and all selected parameters, as well as the camera settings, are stored. Another expert can see the landmarks, and they are listed together with their labels as a preview in the top right cor-

Figure 2: *A tabular overview showing all data sets, where a preview image shows the aneurysm morphology. Filtering masks are provided to define cohorts.*

ner of the corresponding view. Selecting a landmark in the preview loads the corresponding scene.

If ANEULYSIS is started, the user gets access to the main screen, which shows an overview of existing cases, see Figure 2. A preview is shown, generated with our method to calculate optimal views on aneurysms [MEB*17]. Here, the user has three options to proceed, see Figure 1. Firstly, a case can be added, where various metadata for new cases, studies, and aneurysms can be provided. Secondly, we provide configurable filtering masks to define particular cohorts, where study and aneurysm information can be selected, see Figure 2. Thirdly, the user can edit a case, where a summary of metadata and files on the server is displayed. Files can be up- and downloaded to/from the server, or the data can be visualized.

ANEULYSIS provides five visualization modules. The *morphological aneurysm visualization* (MorAVis) module is used to extract and explore morphological descriptors, which are saved in the database, see Section 5.2. Besides, the *combined wall and flow visualization* (CoWaFloVis) module, the *multiple scalar field visualization* (MuScaVis) module and the *comparative tensor visualization* (CoTenVis) module support the visual analysis of wall-related data, see Section 5.3. With the *visual flow exploration* (ViFlEx) module, flow patterns can be visually analyzed, see Section 5.4.

5.2. Visual Exploration of the Aneurysm Morphology

To overcome the error-prone manual extraction of morphological descriptors, an automatic computation is needed that leads to reproducible results. The *MorAVis* module allows an automatic extraction and interactive exploration of morphological descriptors, including the ostium based on a 3D surface representation of the vasculature [MGW*18] (Req. 2). An automatic calculation of these features based on 2D clinical image data would require automatic detection of aneurysms. However, recent approaches [CM16, HBP*14] have still problems with false detections as well as missed detections, and a reliable 2D ostium extraction is also challenging [KAB*04].

5.2.1. Extraction of the Aneurysm Ostium

To identify correlations between morphological descriptors and rupture, many data sets have to be analyzed, which requires a fast descriptor extraction. An important descriptor is the ostium, which can be seen as an imaginary surface that separates the aneurysm from the healthy parent vessel. Thus, the vessel structure without an aneurysm needs to be predicted. Most detection algorithms require a priori knowledge, e.g., the centerline or user interaction [NDSP10]. To avoid such dependencies, we developed an efficient algorithm that automatically calculates the ostium, see Figure 3(a). This can be interactively corrected if necessary. Recently, we extended the ostium detection to multiple aneurysms using a machine learning approach, where a structured report of the morphological descriptors is generated [LMPH19].

5.2.2. Calculation of Morphological Descriptors

Inspired by medical studies, we compute several descriptors using the ostium. They are shown within the 3D vessel surface, which is depicted semi-transparently, and Phong shaded to support shape perception. Each descriptor, such as the diameter of the aneurysm, consists of a starting point and an end point. Their Euclidean distance gives the value of each descriptor. Their start and endpoints are rendered as spheres, and the connecting line is shaded as a tube to improve its perception, see Figure 3(b). For this purpose, we constructed view-aligned quads on the GPU [LGV*15]. The consecutive start- and end points $\mathbf{p}_i$ and $\mathbf{p}_{i+1}$ are used to determine the normalized tangent vector: $\mathbf{t} = \mathbf{p}_{i+1} - \mathbf{p}_i$. With the given view direction $\mathbf{v}$, we calculate the extent of the quad by using the normalized cross-product $\mathbf{e} = \mathbf{v} \times \mathbf{t}$. For every generated quad, we assign a parameter $y \in [-1, 1]$ to define its color: $color = c_{col} \cdot cos(0.5y \cdot \pi)$ in the fragment shader, where c_{col} is set to a specific RGB color for each criterion, which results in a shaded cylinder. The user can activate individual descriptors during the exploration. Moreover, their quantitative values are listed.
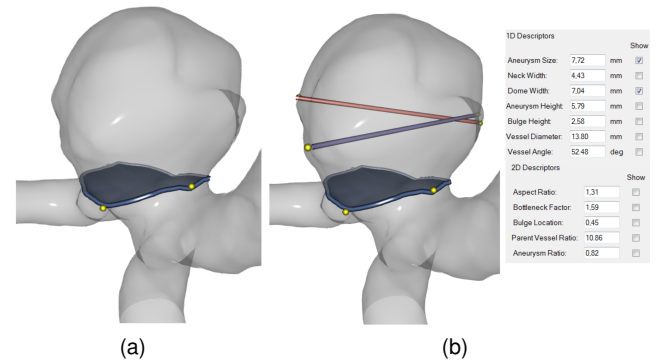

(a) (b)

Figure 3: *Automatic ostium extraction (a). Based on this, morphological descriptors are computed and visualized within the vessel together with their quantitative values (b).*

5.3. Surface-Based Exploration of Aneurysm Data

Depending on the data type, i.e., scalar, vector, or tensor data, three modules allow an interactive exploration of this information by

overcoming limitations of existing visualization approaches. Besides, a capable camera control is crucial to reduce the manual exploration effort, where interesting characteristics can be easily overlooked. Therefore, we developed a method to determine optimized views with two attribute combinations showing potential risk regions [MEB*17]. The automatic determination of appropriate viewpoints is modeled as an optimization problem based on user-defined thresholds of the scalar surface attributes that should be fulfilled. The result is a series of viewpoints over time that can be combined to create an automatic camera movement that gives an overview of suspicious surface regions (Req. 6). It can be activated within the modules, where the results are stored in the database.

5.3.1. MuScaVis Module

The *MuScaVis* module focuses on a simultaneous exploration of multiple scalar fields on the vessel wall to identify correlations between them [MGB*18]. Here, also the homogeneity of attributes is investigated. Experts assume that the thinner the wall and the more inhomogeneous attributes such as WSS or pressure are, the higher the risk of rupture. Vectorial flow information is not shown to reduce the visual complexity.

The *MuScaVis* module combines information and scientific visualization techniques organized in four equally-sized linked views. Brushing and linking aid the user to study risky correlations. The first view comprises a novel 2D plot that shows existing attributes and their correlations over the cardiac cycle, see Figure 4. The plot presents an analogy to a clock, which is reasonable to depict periodic time-dependent data. Along its angle, the simulated time steps are encoded and along the plots radius the existing scalar fields are depicted. For each scalar field, a threshold can be selected. The coloring within the cells represent different surface regions, where the selected thresholds of the scalar fields are fulfilled. With this, interesting surface regions and time steps according to occurring scalar values can be detected without an exhausting exploration in 3D using animations.

Moreover, the user can brush individual regions on the 2D map or the 3D surface, where a 'C' is rendered in the plot center to indicate the 'Custom' region brushing. The aneurysm in Figure 4 exhibits multiple blebs that are brushed. Here, low wall thickness and high WSS, as well as increased pressure, are selected as features. The orange region fulfills all conditions, which indicates a possible rupture-prone area. To explore this region in more detail, the plot segments can be selected, where the selected segment is highlighted. Then, the animation time is set to the selected time step and a contour rendering is activated on the 2D map and the 3D surface to uncover the chosen scalar field.

In the remaining views, the aneurysm data is presented animatedly, representing the cardiac cycle, where the animation time is consistent between the views. The second view shows a matrix-based visualization that enables a comparison of data sets (Req. 3). Each entry of the matrix represents a combination of two scalar fields, see Figure 5. Statistical plots are shown that give an overview of the distribution of scalar quantities. Thereby, the upper triangle matrix represents the first case, e.g., a non-treated case. In the lower triangle matrix, another case can be loaded, e.g., a treated aneurysm. The non-diagonal entries of the matrix present scatter-
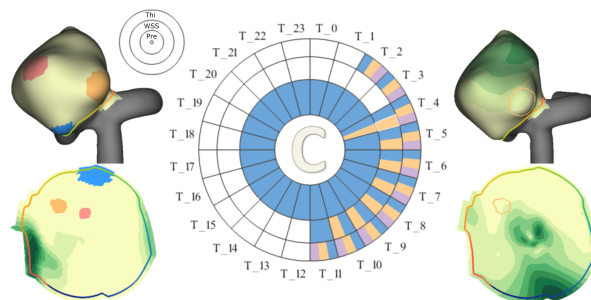

Figure 4: *Brushing of risky regions used to color the plot depending on a selected threshold for each attribute. A contour rendering is activated for a chosen plot segment.*
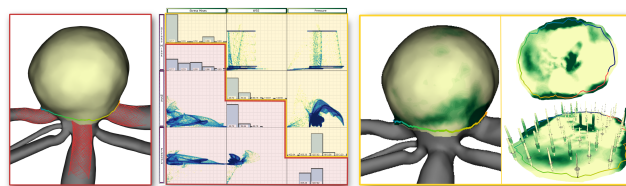

Figure 5: *Comparison of a pre- and post-treated aneurysm data set using statistical plots. By inserting a stent, the forces acting on the vessel wall, such as WSS and pressure, were significantly reduced.*

plots for each scalar field combination. The diagonal entries are used for a histogram that shows occurring values of the corresponding scalar field. To show the histograms for both data sets, the diagonal entries are split and display on top the histograms of the first case and below the values of the second case.

Aneurysms could have irregularly deformed shapes, which complicates the simultaneous exploration of scalar quantities in 3D. Thus, we provide a 3D aneurysm visualization in the third view as well as a 2D aneurysm map, which is displayed in the fourth view. The 2D map shows a simplified representation of the aneurysm morphology and gives a fast overview about the distribution of a chosen scalar quantity without any occlusions (Req. 4). Due to linking options, both views allow a detailed exploration of high-risk wall regions over time. In case of post-treated data, we provide a depiction of existing stent configurations. For generating the map, the aneurysm surface is parametrized to the 2D domain, where the ostium is color-coded on the 3D mesh and the map to establish a spatial correlation between both views, see Figure 5(right). We used *spectral conformal parameterization* (SCP) [MTAD08] to compute the 2D map. To reduce the length distortion, we further process the vertices on the 2D domain according to Zayer et al. [ZRS05].

Furthermore, we provide several techniques to analyze two scalar attributes simultaneously on the 2D map as well as on the 3D surface to investigate possible rupture-prone correlations. The first option is a hatching approach, which discretizes the data range into four patterns to give an overview of regions with high and low values. For a more detailed analysis of specific surface regions, we developed a checkerboard visualization that allows a simultaneous exploration of two attributes by generating a linear transition be-
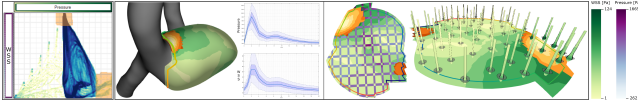
Figure 6: *An aneurysm that was assessed as less rupture-prone based on morphological features. Using the MuScaVis module, the rupture site could be identified.*

tween them, see Figure 6. Since, we want to display the checkerboard texture on the 2D map as well as on the 3D surface, a conformal parametrization for the map generation is needed. In addition, violin glyphs can be activated on the map showing the temporal behavior of two selected scalar attributes. For this purpose, we create a cylinder with a fixed number of points for the radius and the height. The first attribute is depicted using a linear color scale. For visualizing the second attribute, every point of the cylinder is shifted along the normal such that the radius corresponds to the specific scalar value. A disc indicates the current time at the corresponding glyph height. The glyphs are placed at regular grid points. Additionally, the user can add glyphs at specific regions by clicking on the map to analyze quantities at different points.

To more easily detect regions of interesting attribute combinations, we provide a clustering scheme that results in surface regions with similar scalar values. In contrast to Glaßer et al. [GLH*14], who defined a fixed combination of WSS and wall thickness for a single time step, different combinations over time are possible. To support the process of combining attributes for clustering, we assist the experts with different facilities. First, the expert can set individual weights for each attribute. Furthermore, attributes can be normalized to the range $[0, 1]$, which is activated as a default value. Moreover, some quantities might be more interesting if low values occur instead of high values, e.g., wall thickness. The expert may rather be interested in a cluster that exhibits high WSS and low wall thickness. For this purpose, an attribute can be inverted. The clustering yields non-overlapping regions, where each surface point is assigned to a cluster. To assess the homogeneity of regions, a risk factor is determined for each cluster, which can be color-coded on the 2D map and the 3D surface. Inhomogeneous regions show a larger number of clusters with strongly varying risk values, whereas homogeneous regions exhibit fewer clusters with similar risk values.

The analysis of scalar quantities requires brushing and linking facilities that allow the user to explore the aneurysm morphology in interesting regions. In case the scatterplot shows interesting combinations, the expert may analyze the morphological attributes in 3D or on the 2D map. Therefore, the user can brush regions in the scatterplot, which are highlighted immediately on the 3D surface and 2D map, see Figure 6. The brush radius can be controlled with the mouse wheel. The user can also mark regions on the 3D surface or the 2D map and the corresponding regions in the other views are highlighted. Thus, linking between the scatterplot, the 2D map and the surface mesh is simplified.

5.3.2. CoWaFloVis Module

Besides the exploration of multiple scalar fields on the vessel wall, their interplay with the internal blood flow is an important aspect to assess the rupture risk and treatment options. The *CoWaFloVis* module allows a simultaneous visualization of scalar and vectorial data [MVB*17a]. For visualizing the scalar information, techniques from the *MuScaVis* module, such as the hatching or checkerboard visualization, can be used. In addition, the 2D aneurysm map is reused, which provides a clear overview of attributes. Similar to the *MuScaVis* module, brushing and linking techniques are provided to facilitate the correlation between both views.

Besides the internal blood flow, the wall deformation due to the heart beat is represented as a vector field. The wall deformation and thickness is depicted by an extended wall visualization on the 3D aneurysm surface, see Figure 7(a). The wall visualization comprises two wall layers, an inner and outer wall, where the outer wall is depicted semitransparently and the distance between two layers shows the wall thickness. Additionally the wall layers deform to show the wall deformation.

Path lines represent the inner blood flow, which are visualized by arrow glyphs and by color. This approach allows an easy interpretation of the speed. If the animation pauses, the length of the depicted path line part corresponds to the speed. Furthermore, another value, e.g., the pressure can be visualized by a color scheme.
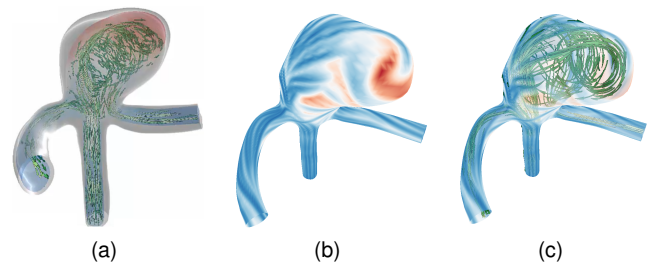

Figure 7: *In 3D both walls with blood flow are displayed* (a). *On the inner wall, e.g., the NWF can be color-coded. Blue areas indicate that flow comes close to the wall, whereas in red regions the path lines have a greater distance to the wall* (b). *The path lines follow the blue stripes on the wall that display NWF regions* (c).

Moreover, the *near-wall flow* (NWF) can be explored. Therefore, we determine for each vertex of the surface mesh the nearest path line point using the Euclidean distance. Finally, we took for each vertex the minimum overall path line points and time steps to represent the global near-wall flow. This enables a visualization that depicts the trace of the path lines over time. Figure 7(b) and 7(c) show the NWF using a color-coding. Blue regions indicate flow that comes close to the wall, whereas in the red regions the flow has a greater distance to the wall, based on the path lines. Regions, where the flow is more distant to the wall, indicate that there are thickenings of the inner wall due to the formation of a thrombus or inflammation processes stated by our neuroradiological experts.

5.3.3. CoTenVis Module

Tensor data describe structural stresses in the walls induced by the blood flow, which influence the aneurysm evolution and rupture. However, the obtained data are very complex. At each vertex on the aneurysm wall, a tensor is calculated, represented as a 3×3 symmetric matrix, that describes stresses within the aneurysm wall. Moreover, the wall is divided into an inner and outer layer, where for each vertex on both walls a tensor is available.

The analysis of structural stresses without a reduction of the tensor data to a scalar field was not possible so far. Therefore, we developed the *CoTenVis* module, which provides the first integrated visualization of stress tensors as well as scalar and vector data to study possible correlations between these different forces [MVB*17b] (Req. 5). We developed four glyph designs to qualitatively and quantitatively depict tensor information, see Figure 8. They enable a comparative tensor visualization between the inner and outer wall, which is essential to localize rupture-prone areas. The glyph visualization is based on a details-on-demand strategy, facilitating the analysis of local stress configurations. The interactive and simultaneous exploration of these different information takes place on a 3D aneurysm depiction.

The first method is a kite-shaped glyph, where the glyph is oriented along the first eigenvector of the corresponding tensor and scaled by the first two eigenvalues. The second technique is a superquadric visualization, which is also oriented and scaled based on the eigenvectors and eigenvalues of the tensor. The third technique are streamlines on the surface along the first eigenvector, which show the tensor characteristics on the inner and outer wall. The fourth method is a scatterplot, which gives a quantitative overview of tensor information within a specific surface region. The different glyph designs provide an overview of the data and also allow a detailed analysis of the tensor properties.
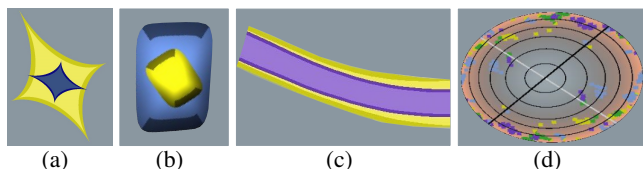

Figure 8: *Four glyph designs to visualize stress tensors. We compared kite-shaped glyphs* (a), *superquadrics* (b), *streamlines* (c), *and scatterplots* (d) *to depict tensor information on the inner and outer vessel wall simultaneously.*

5.4. Visual Exploration of Aneurysm Flow Patterns

Qualitative flow patterns seem to have a decisive influence on the development and progression of aneurysms. A flow pattern is a set of flow-representing integral lines that have a similar course within the aneurysm. To assess the influence of flow patterns on rupture and treatment success, medical studies manually classified them according to their *complexity* and *temporal stability* in ruptured and non-ruptured aneurysms. The more complex and unstable types correlated with rupture. Such an analysis is time-consuming and subjective, where flow patterns more distant to the wall are
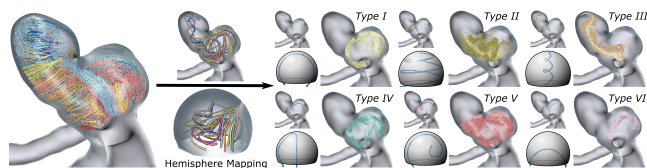

Figure 9: *Automatic flow pattern classification. One of six (I-VI) pre-defined types is assigned to each pattern.*

easily overlooked. However, to uncover correlations between flow patterns and the aneurysm state, the classifications of different data sets should be comparable. This requires an objective and reproducible classification according to defined criteria, which is ensured by the *ViFlEx* module [MOJB*18] (Req. 2).

First, flow-representing path lines are grouped to get groups of lines with similar flow behavior, which represents the flow patterns. For this purpose, we developed an automatic clustering approach based on the mean distance between path lines that directly incorporates their temporal component and is not dependent on pre-defined data [MVPL18]. If a flow pattern occurs, decays and reoccurs during the cardiac cycle, several clusters are generated. This is required since the stability of flow patterns is an important criterion in medical studies to predict the rupture risk [CMWP11]. Besides, a representative is computed for each cluster.

Second, the flow patterns are automatically classified according to pre-defined types. This is based on a novel mapping of the aneurysm surface to a hemisphere by calculating polar-based coordinates that circumvent restrictions of existing techniques in case of a non-convex aneurysm shape. Then, the polar-based coordinates are assigned to the points of the cluster representatives. Each representative is classified according to six pre-defined templates based on the study by Cebral et al. [CMWP11], see Figure 9. Due to the anatomic diversity, a cluster could be dissimilar to all pre-defined types or two types may have similar values. Therefore, new flow types can be added by the user. Besides, we introduce a detail-on-demand approach that creates a visual transition from the cluster representative over an enclosing surface to the associated lines to support the spatial perception of flow patterns. However, a very irregularly deformed aneurysm surface complicates the exploration of flow patterns including the recognition of the calculated flow types. Manual rotations are necessary to perceive the behavior of individual patterns. Therefore, the representatives can also be visualized as tubes within the hemisphere, which provides a more simplified representation of flow patterns (Req. 4). If all representatives are depicted simultaneously, the hemisphere-based visualization provides a fast overview of existing flow patterns. For further analysis, the user can select individual representatives or groups of them having the same flow type.

6. Results

This section gives an overview of the implementation of ANEULYSIS and provides an informal assessment with user feedback and case study that demonstrate the analysis capabilities of the tool.

6.1. Implementation

ANEULYSIS is a *Windows Forms application*, which is a toolkit of the *Microsoft .NET Framework* to design *GUIs* and written in C#. For the database, a Microsoft SQL Server is used, where the *Microsoft .NET Framework* provides extensive functionality to built up a connection between the FTP-server, the database and the GUI of ANEULYSIS. For rendering, the *open toolkit library* (OpenTK) is used, a C# graphics library that provides access to graphics tools contained in the *open graphics library* (OpenGL). Moreover, OpenTK provides multiple helpful data types such as 3D vectors, 4D vectors, and matrices with specialized functionality for specific dimensions, such as cross-product for 3D. No commercial or GPL libraries are used. ANEULYSIS requires a graphics card that supports OpenGL 4.3. As operating systems, we tested Windows 7/8/10. Using ANEULYSIS is exclusively allowed for research purposes, since it has no CE certification or FDA approval.

6.2. Case Study

We used 13 data sets (D1-D13) to evaluate if ANEULYSIS supports risk assessment and treatment decisions. We asked four radiologists to assess the risk of rupture and the need for treatment based on morphological characteristics extracted with the *MorAVis* module. Note that they were not informed about the states of the aneurysms (ruptured or non-ruptured). The non-ruptured cases included two smaller (diameter $\leq 7\,mm$), morphologically inconspicuous aneurysms (D1 and D2) for which a low risk was predicted. In contrast, the doctors were unsure for D3. Only considering the diameter ($8\,mm$), they advised treatment based on the clinical guidelines, but there were no blebs, so that the aneurysm could first be observed. For the remaining five non-ruptured cases (D4-D8), the doctors estimated an increased risk and advised to treat them due to the larger diameter (about $10\,mm$) and additional blebs on the aneurysm. Similar, they predicted an increased risk for the ruptured cases D9, D10 and D11 due to blebs. For the remaining two ruptured cases, D12 and D13, they were again more uncertain. Similar to D3, D12, with a size of $8\,mm$, reaches the limit for a treatment recommendation, but has a morphology that seems rather low risk. D13 is even smaller ($5.3\,mm$), but the morphological features of the wall seem to be a little more striking because the wall appears slightly bumpy, see Figure 6.

Afterwards, the remaining modules were used to explore wall and flow-related features, where we summarized the major features of ANEULYSIS and corresponding exploration tasks in Table 1. We observed slightly different workflows for risk analysis and treatment assessment. A patient-specific risk analysis was declared to be extremely important for small aneurysms or aneurysms without blebs, such as D1-D3 as well as D12-D13, for which a low risk is predicted based on morphological characteristics. The goal is to find risky correlations between blood flow behavior and the harmless appearing vessel wall.

For this purpose, first the *MuScaVis* module was used to explore correlations between scalar wall and flow attributes. Here, one radiologist starts with the automatic camera animation to get an overview of risky wall regions. The remaining experts initially used the circle plot to identify time steps in which the scalar fields exceed risky thresholds. The one who used the animation described this feature as an easy way to get a quick overview of important wall regions (meet Req. 6). The remaining experts criticized that the automatic viewpoint calculation currently only takes two scalar fields into account. Therefore they prefer to use the circle plot.

The definition of corresponding thresholds was based on experience, with particular interest in thin wall regions with high WSS and pressure values. Since the colored regions in the circular plot could represent individual outliers, the scatterplots and histograms were also used to examine the scalar distributions, and the 2D map with the glyphs to brush conspicuous regions. Afterwards, they activated the statistical diagrams that show the temporal behavior of scalar fields within the brushed regions to analyze these areas more quantitatively. In addition, they used the hatching and checkerboard visualization to explore the behavior of a second scalar field on the map. However, we could not identify a clear preference for either of the two methods. With this, increased WSS values are detected on the ostium region, which was the rupture area of D13, see Figure 6. So a risk analysis based on morphological criteria was not appropriate.

In addition, they used the *ViFlex* module to analyze the complexity of the flow patterns, where complex vortical and temporally unstable flow patterns were found. Similar areas were found for D3 and D12, so the experts are more confident that these cases are more risky, finding the rupture site of D12. D2 shows similar WSS values at the ostium region as D13, however the blood flow patterns are more stable over time and show no complex flow behavior. So the experts would first observe the aneurysm. For D1 no risky wall regions or flow patterns were found, so the experts maintained their opinion of a smaller risk.

For risky appearing aneurysms, the treatment planning workflow follows. The experts here focused their analysis on regions for which they have already identified an increased risk using the *MorAVis* module. First, the circle plot was used to analyze correlations of scalar attributes within the suspicious regions. Moreover, the scatter plots and histograms were used to compare attribute distributions before and after treatment. Based on this depiction, the experts could easily assess how the scalar distributions are changing depending on the selected stent (meet Req. 3). If there is no clear changing of, e.g., the WSS values, the selected stent type or its location is probably not appropriate to prevent aneurysm inflow. Furthermore, the *ViFlex* module was used to explore if flow patterns are changing after treatment. For D11, four different stent configurations were simulated, where the experts decide for the fourth to be the best. This stent reduced pressure and WSS acting on the vessel wall and suppressed the complex flow within the aneurysm.

6.3. User Feedback

In addition to medical experts, ANEULYSIS was evaluated by two CFD experts, whereby we summarize the feedback from both user groups. Both groups appreciated the structured management and the guided exploration process. New data sets can be easily added and edited (meet Req. 1). The ability to save and load exploration results allows for collaborative analysis of data sets by experts from different domains (meet Req. 7). The radiologists described

Task	Features	Module
Explore aneurysm morphology	Compute morphological descriptors	MorAVis module [MGW*18] (Sec. 5.2)
Show suspicious surface regions	Automatic camera animations	Optimal viewpoints [MEB*17] (Sec. 5.3)
Show correlations between two scalar fields	Checkerboard	MuScaVis module [MGB*18] (Sec. 5.3.1)
	Hatching	MuScaVis module [MGB*18] (Sec. 5.3.1)
Overview of temporal behavior of scalar fields	Automatic camera animations	Optimal viewpoints [MEB*17] (Sec. 5.3)
	Circular Plot	MuScaVis module [MGB*18] (Sec. 5.3.1)
	Violin Glyphs	MuScaVis module [MGB*18] (Sec. 5.3.1)
Explore wall deformation	Visualization of wall layers	CoWaFloVis module [MVB*17a] (Sec. 5.3.2)
Explore complexity of flow patterns	Flow pattern classification + hemisphere-based visualization	ViFlEx module [MOJB*18] (Sec. 5.4)
Explore attributes on flow patterns	Detail-on-demand visualization	ViFlEx module [MOJB*18] (Sec. 5.4)
Compare data sets	Statistical plot matrix	MuScaVis module [MGB*18] (Sec. 5.3.1)
Overview of tensor main directions	Streamline glyphs	CoTenVis module [MVB*17b] (Sec. 5.3.3)
Detailed analysis of tensor information	Kite glyphs	CoTenVis module [MVB*17b] (Sec. 5.3.3)
	Superquadrics	CoTenVis module [MVB*17b] (Sec. 5.3.3)
Explore distribution of tensor directions	Scatterplot glyphs	CoTenVis module [MVB*17b] (Sec. 5.3.3)

Table 1: *Tasks and major features of* ANEULYSIS *used by our domain experts as well as the corresponding module.*

the *MorAVis*, *MuScaVis* and *ViFlEx* modules as the most important components of the visual analysis. The automatic calculation of morphological descriptors was considered very helpful, as it saves time and avoids measurement errors (meet Req. 2). Related to this, they commented that the *ViFlEx* module allows a faster and objective analysis of suspicious flow patterns in clinical discussions by providing an automatic classification and efficient exploration techniques (meet Req. 2). Basically the 3D aneurysm view was used for the evaluation of the flow patterns. The hemisphere-based flow pattern representation was described as an interesting overview, but was not absolutely necessary for the analysis. Therefore, we will hide this presentation again in the future. In addition, they appreciated the 2D map as simplified morphology representation as it strongly reduces the manual exploration effort of the time-dependent scalar fields (meet Req. 4). It is no longer necessary to constantly rotate the 3D aneurysm to get an overview of the data.

The visualization of the wall deformation with the help of the *CoWaFloVis* module plays a less important role for them, because the wall deformation in the cerebral vessels is rather small. Furthermore, they were not familiar with the concept of stress tensors and the associated visualizations still seemed quite abstract to them and did not influence their risk assessment or treatment recommendation. In contrast, the combination of the other three modules improve the aneurysm risk analysis and treatment decision compared to the previous clinical procedure as rupture sites of aneurysms as well as appropriate stent scenarios could detected in the case study.

The CFD experts, on the other hand, emphasized the importance of the *CoWaFloVis* and *CoTenVis* modules for their research. The integration of the wall deformation is an important step to improve the accuracy of flow simulation, where the *CoWaFloVis* module helps to analyze the results. In addition, the *CoTenVis* module allows visual exploration of the tensor properties at different wall layers for the first time. This is important to validate CFD results and to get a better understanding of the forces acting on the wall (meet Req. 5). However, it turned out that the glyphs are differ-

ently suitable depending on the task, see Table 1. The streamlines provide a first overview of the tensor main directions on both walls. Since, the streamlines could lead to occlusion problems, other techniques such as superquadrics and kites were preferred for a more detailed analysis of the tensor components. For the rotating kites, they used the metaphor of a compass, whereby regions with strong local directional changes could be recognized immediately. The scatterplots are most suitable to analyze the tensor data quantitatively within a surface region, whereas the other techniques allow a qualitative analysis. They allow a quantification of the homogeneity of the tensor main directions. Strong inhomogeneous regions paired with suspicious scalar values such as a high WSS could be a rupture-prone criterion.

In addition, both user groups appreciated the calculation of optimal views and animations to improve the exploration of multiple scalar fields on the wall. This reduces the manual exploration effort. The generation of a report on the basis of morphological criteria was described by the radiologists as an important tool to support documentation. In future, however, the results from the other modules should also be integrated into this report.

7. Conclusion and Future Work

This paper described ANEULYSIS – a system to manage and visually explore aneurysms developed in close cooperation with medical and CFD experts. It shows the dynamic interaction between the wall and flow to get a deeper understanding of their growth and rupture. *Aneulysis* is focused on clinically essential aspects, such as to find an optimal treatment and supports the communication between engineers and physicians, e.g., in investigating how changes in flow patterns after treatment are related to its success. To further promote the exploration of aneurysms, we will making the source code of the five visualization modules freely available on an open access repository.

To further improve the decision-making process, the comparison of data sets should receive more attention in the future. Meth-

ods are needed that allow a comparison of multiple instances of dynamic data, which is challenging with existing techniques. The comparison of two time-dependent vector fields along with the vascular anatomy and different treatment options would benefit from detection of corresponding and unique features. Furthermore, multiple aneurysms occur in about one-fifth of aneurysm patients and require specific analysis methods, since they may require several treatment cycles. The physician has to decide which aneurysm should be treated first and how does treatment affect the remaining aneurysms? Therefore, ANEULYSIS should be extended in the future to better support the analysis of multiple aneurysms. This also includes a stronger focus on aneurysm treatment, integrating interaction techniques to plan treatment. Moreover, the result reporting could be improved by integrating animations into the report [PM20]. In addition, we plan to integrate the exploration of other vascular pathologies, such as vessel narrowing, also in other vessels, such as the aorta, where the exploration of wall and flow properties plays also an important role. Many concepts of ANEULYSIS could also be applied in such scenarios.

Acknowledgments

References

[AGL05]   AHRENS J., GEVECI B., LAW C.: Paraview: An end-user tool for large data visualization. *The visualization handbook 717* (2005). 2

[BDJ17]   BERG P., DARÓCZY L., JANIGA G.: Virtual stenting for intracranial aneurysms: A risk-free, patient-specific treatment planning support for neuroradiologists and neurosurgeons. In *Computing and visualization for intravascular imaging and computer-assisted stenting.* 2017, pp. 371–411. 3

[CDJ*17]   CATTANEO G. F. M., DING A., JOST T., LEY D., MÜHL-BENNIGHAUS R., YILMAZ U., KÖRNER H., REITH W., SIMGEN A.: In vitro, contrast agent-based evaluation of the influence of flow diverter size and position on intra-aneurysmal flow dynamics using syngo iflow. *Neuroradiology 59*, 12 (2017), 1275–83. 2

[CM16]   CHANDRA A., MONDAL S.: Amalgamation of iterative double automated thresholding and morphological filtering: a new proposition in the early detection of cerebral aneurysm. *Multimed Tools Appl* (2016). 5

[CMWP11]   CEBRAL J. R., MUT F., WEIR J., PUTMAN C. M.: Association of hemodynamic characteristics and cerebral aneurysm rupture. *Am J Neuroradiol 32*, 2 (2011), 264–70. 1, 2, 3, 8

[DTM*08]   DHAR S., TREMMEL M., MOCCO J., KIM M., YAMAMOTO J., SIDDIQUI A. H., HOPKINS L. N., MENG H.: Morphology parameters for intracranial aneurysm rupture risk assessment. *J Neurosurg 63*, 2 (2008), 185–97. 2

[GLH*14]   GLASSER S., LAWONN K., HOFFMANN T., SKALEJ M., PREIM B.: Combined Visualization of Wall Thickness and Wall Shear Stress for the Evaluation of Aneurysms. *IEEE Trans Vis Comput Graph* (2014), 2506–15. 7

[GLvP*12]   GASTEIGER R., LEHMANN D. J., VAN PELT R., JANIGA G., BEUING O., VILANOVA A., THEISEL H., PREIM B.: Automatic Detection and Visualization of Qualitative Hemodynamic Characteristics in Cerebral Aneurysms. *IEEE Trans Vis Comput Graph 18(12)*, 12 (2012), 2178–87. 2

[GNBP11]   GASTEIGER R., NEUGEBAUER M., BEUING O., PREIM B.: The FLOWLENS: A Focus-and-Context Visualization Approach for Exploration of Blood Flow in Cerebral Aneurysms. *IEEE Trans Vis Comput Graph 17*, 12 (2011), 2183–92. 2

[GRC*18]   GROEN D., RICHARDSON R. A., COY R., SCHILLER U. D., CHANDRASHEKAR H., ROBERTSON F., COVENEY P. V.: Validation of patient-specific cerebral blood flow simulation using transcranial doppler measurements. *Front Physiol 9* (2018), 721. 2

[GSK*12]   GOUBERGRITS L., SCHALLER J., KERTZSCHER U., VAN DEN BRUCK N., POETHKOW K., PETZ C., ET AL.: Statistical wall shear stress maps of ruptured and unruptured middle cerebral artery aneurysms. *J R Soc Interface 9*, 69 (2012), 677–88. 2

[HBP*14]   HENTSCHKE C. M., BEUING O., PAUKISCH H., SCHERLACH C., SKALEJ M., TÖNNIES K. D.: A system to detect cerebral aneurysms in multimodality angiographic data sets. *J Med Phys 41*, 9 (2014). 5

[JBB*13]   JANIGA G., BERG P., BEUING O., NEUGEBAUER M., GASTEIGER R., PREIM B., ROSE G., SKALEJ M., THÉVENIN D.: Recommendations for accurate numerical blood flow simulations of stented intracranial aneurysms. *Biomed Eng-Biomed Te 58*, 3 (2013), 303–14. 1, 3

[KAB*04]   KARMONIK C., ARAT A., BENNDORF G., AKPEK S., KLUCZNIK R., MAWAD M. E., STROTHER C. M.: A technique for improved quantitative characterization of intracranial aneurysms. *Am J Neuroradiol 25*, 7 (2004), 1158–61. 5

[LAM*13]   LARRABIDE I., AGUILAR M., MORALES H., GEERS A., KULCSÁR Z., RÜFENACHT D., FRANGI A.: Intra-aneurysmal pressure and flow changes induced by flow diverters: relation to aneurysm size and shape. *Am J Neuroradiol 34*, 4 (2013), 816–22. 2

[LBM12]   LAURIC A., BAHAROGLU M. I., MALEK A. M.: Ruptured status discrimination performance of aspect ratio, height/width, and bottleneck factor is highly dependent on aneurysm sizing methodology. *J Neurosurg 71*, 1 (2012), 38–46. 2

[LGP14a]   LAWONN K., GASTEIGER R., PREIM B.: Adaptive Surface Visualization of Vessels with Animated Blood Flow. *Comput Graph Forum 33(8)* (2014), 16–27. 2

[LGP14b]   LAWONN K., GÜNTHER T., PREIM B.: Coherent view-dependent streamlines for understanding blood flow. In *EuroVis - Short Papers* (2014). 2

[LGV*15]   LAWONN K., GLASSER S., VILANOVA A., PREIM B., ISENBERG T.: Occlusion-free blood flow animation with wall thickness visualization. *IEEE Trans Vis Comput Graph 22*, 1 (2015), 728–37. 2, 5

[LMPH19]   LAWONN K., MEUSCHKE M., PREIM B., HILDEBRNADT K.: Automatic Detection and Segmentation of Multiple Aneurysms. *Comput Graph Forum 38(3)* (2019), 413–25. 5

[LP16]   LAWONN K., PREIM B.: *Feature Lines for Illustrating Medical Surface Models: Mathematical Background and Survey.* Springer Verlag, 2016, ch. Visualization in Medicine in Life Sciences III, pp. 93–132. 2

[LSBP17]   LAWONN K., SMIT N., BÜHLER K., PREIM B.: A Survey on Multimodal Medical Data Visualization. In *Comput Graph Forum* (2017). 2

[LVPI18]   LAWONN K., VIOLA I., PREIM B., ISENBERG T.: A Survey of Surface-Based Illustrative Rendering for Visualization. *Comput Graph Forum 37(6)* (2018), 205–34. 2

[MEB*17]   MEUSCHKE M., ENGELKE W., BEUING O., PREIM B., LAWONN K.: Automatic Viewpoint Selection for Exploration of Time-dependent Cerebral Aneurysm Data. In *Proc. of BVM* (2017), pp. 352–57. 5, 6, 10

[MGB*18]   MEUSCHKE M., GÜNTHER T., BERG P., WICKENHÖFER R., PREIM B., LAWONN K.: Visual Analysis of Aneurysm Data using Statistical Graphics. *IEEE Trans Vis Comput Graph 25*, 1 (2018), 997–1007. 6, 10

[MGW*18] MEUSCHKE M., GÜNTHER T., WICKENHÖFER R., GROSS M., PREIM B., LAWONN K.: Management of cerebral aneurysm descriptors based on an automatic ostium extraction. *IEEE Comput Graph Appl 38*, 3 (2018), 58–72. 5, 10

[MNP11] MOENCH T., NEUGEBAUER M., PREIM B.: Optimization of vascular surface models for computational fluid dynamics and rapid prototyping. In *Second International Workshop on Digital Engineering* (2011), pp. 16–23. 3

[MOJB*18] MEUSCHKE M., OELTZE-JAFRA S., BEUING O., PREIM B., LAWONN K.: Classification of blood flow patterns in cerebral aneurysms. *IEEE Trans Vis Comput Graph* (2018). 8, 10

[MTAD08] MULLEN P., TONG Y., ALLIEZ P., DESBRUN M.: Spectral conformal parameterization. In *Proc. of Symp Geom Process* (2008), pp. 1487–94. 6

[MVB*17a] MEUSCHKE M., VOSS S., BEUING O., PREIM B., LAWONN K.: Combined Visualization of Vessel Deformation and Hemodynamics in Cerebral Aneurysms. *IEEE Trans Vis Comput Graph 23*, 1 (2017), 761–70. 7, 10

[MVB*17b] MEUSCHKE M., VOSS S., BEUING O., PREIM B., LAWONN K.: Glyph-based Comparative Stress Tensor Visualization in Cerebral Aneurysms. *Comput Graph Forum 36*, 3 (2017), 99–108. 8, 10

[MVPL18] MEUSCHKE M., VOSS S., PREIM B., LAWONN K.: Exploration of Blood Flow Patterns in Cerebral Aneurysms during the Cardiac Cycle. *Computers & Graphics 72* (2018), 12–25. 8

[NBR*18] NARATA A. P., BLASCO J., ROMAN L. S., MACHO J. M., FERNANDEZ H., MOYANO R. K., WINZENRIETH R., LARRABIDE I.: Early results in flow diverter sizing by computational simulation: quantification of size change and simulation error assessment. *Operative Neurosurgery 15*, 5 (2018), 557–66. 2

[NDSP10] NEUGEBAUER M., DIEHL V., SKALEJ M., PREIM B.: Geometric Reconstruction of the Ostium of Cerebral Aneurysms. In *VMV* (2010), pp. 307–14. 5

[NGB*09] NEUGEBAUER M., GASTEIGER R., BEUING O., DIEHL V., SKALEJ M., PREIM B.: Map displays for the analysis of scalar data on cerebral aneurysm surfaces. In *Comput Graph Forum* (2009), vol. 28 (3), pp. 895–902. 2

[NLB*13] NEUGEBAUER M., LAWONN K., BEUING O., BERG P., JANIGA G., PREIM B.: AmniVis - A System for Qualitative Exploration of Near-Wall Hemodynamics in Cerebral Aneurysms. *Comput Graph Forum 32(3)* (2013), 251–60. 2

[OJCJP16] OELTZE-JAFRA S., CEBRAL J. R., JANIGA G., PREIM B.: Cluster Analysis of Vortical Flow in Simulations of Cerebral Aneurysm Hemodynamics. *IEEE Trans Vis Comput Graph 22(1)* (2016), 757–66. 2

[OJMN*19] OELTZE-JAFRA S., MEUSCHKE M., NEUGEBAUER M., SAALFELD S., LAWONN K., JANIGA G., HEGE H.-C., ZACHOW S., PREIM B.: Generation and Visual Exploration of Medical Flow Data: Survey, Research Trends and Future Challenges. *Comput Graph Forum 38 (1)* (2019), 87–125. 2

[OLK*14] OELTZE S., LEHMANN D. J., KUHN A., JANIGA G., THEISEL H., PREIM B.: Blood Flow Clustering and Applications in Virtual Stenting of Intracranial Aneurysms. *IEEE Trans Vis Comput Graph 20(5)* (2014), 686–701. 2

[PM20] PREIM B., MEUSCHKE M.: A survey of medical animations. *Computers & Graphics 90* (2020), 145–168. 11

[SAC*13] SANCHEZ M., AMBARD D., COSTALAT V., MENDEZ S., JOURDAN F., NICOUD F.: Biomechanical assessment of the individual risk of rupture of cerebral aneurysms: a proof of concept. *Ann Biomed Eng 41*, 1 (2013), 28–40. 3

[Sch97] SCHÖBERL J.: Netgen an advancing front 2d/3d-mesh generator based on abstract rules. *Comput Vis Sci 1*, 1 (1997), 41–52. 3

[SLG15] SU H., LOU W., GU J.: Clinical values of hemodynamics assessment by parametric color coding of digital subtraction angiography before and after endovascular therapy for critical limb ischaemia. *Chin Med J 95*, 37 (2015), 3036–40. 2

[SS06] SALZBRUNN T., SCHEUERMANN G.: Streamline Predicates. *IEEE Trans Vis Comput Graph 12*, 6 (2006), 1601–12. 2

[Ste11] STEINMETZ H.: Unrupturierte intrakranielle aneurysmen. *Der Nervenarzt 82*, 10 (2011), 1343–50. 1

[THQ*16] TAO J., HUANG X., QIU F., WANG C., JIANG J., SHENE C.-K., ZHAO Y., YU D.: VesselMap: A web interface to explore multivariate vascular data. *Computers & Graphics* (2016). 2

[VLR*08] VALENCIA A., LEDERMANN D., RIVERA R., BRAVO E., GALVEZ M.: Blood flow dynamics and fluid–structure interaction in patient-specific bifurcating cerebral aneurysms. *Int J Numer Meth FL 58*, 10 (2008), 1081–1100. 4

[vPGL*14] VAN PELT R., GASTEIGER R., LAWONN K., MEUSCHKE M., PREIM B.: Comparative Blood Flow Visualization for Cerebral Aneurysm Treatment Assessment. *Comput Graph Forum 33(3)* (2014), 131–40. 2

[vPJtHRV12] VAN PELT R., JACOBS S., TER HAAR ROMENY B., VILANOVA A.: Visualization of 4D Blood-Flow Fields by Spatiotemporal Hierarchical Clustering. *Comput Graph Forum 31*, 3pt2 (2012), 1065–74. 2

[ZMSL13] ZENTENO M., MOSCOTE-SALAZAR L. R., LEE A.: Roles and rules of syngo iflow in neuroendovascular procedures. *Romanian Neurosurgery* (2013), 305–8. 2

[ZRS05] ZAYER R., RÖSSL C., SEIDEL H.-P.: Discrete tensorial quasi-harmonic maps. In *Proc. of IEEE Shape Modeling and Applications* (2005), pp. 276–85. 6